Y.-T. Lin and T. F. Duda: JASA Express Letters [http://dx.doi.org/10.1121/1.4730328] Published Online 3 July 2012

A higher-order split-step Fourier parabolic-equation sound propagation solution scheme

Ying-Tsong Lin[a] **and Timothy F. Duda**
Applied Ocean Physics and Engineering Department, Woods Hole Oceanographic Institution, Woods Hole, Massachusetts 02543
ytlin@whoi.edu, tduda@whoi.edu

Abstract: A three-dimensional Cartesian parabolic-equation model with a higher-order approximation to the square-root Helmholtz operator is presented for simulating underwater sound propagation in ocean waveguides. The higher-order approximation includes cross terms with the free-space square-root Helmholtz operator and the medium phase speed anomaly. It can be implemented with a split-step Fourier algorithm to solve for sound pressure in the model. Two idealized ocean waveguide examples are presented to demonstrate the performance of this numerical technique.

PACS numbers: 43.20.Bi, 43.30.Bp [WS]
Date Received: March 29, 2012 **Date Accepted:** June 5, 2012

1. Introduction

The parabolic-equation (PE) approximation, first introduced by Tappert (1974b), has been shown to be an effective numerical technique for modeling underwater sound propagation in the ocean. This technique transforms the Helmholtz wave equation into a one-way wave equation that can be solved by a variety of marching algorithms with the range being the evolution variable. Among those algorithms, the split-step Fourier method (Tappert, 1974a) is most efficient for three-dimensional (3D) cases, because one can employ the fast Fourier transform to calculate the second-order spatial derivatives of the pressure field. In this method, one complete marching step of the solution is split into two sub-steps to sequentially, not simultaneously, solve for free space propagation and phase anomaly. Because of the sequential splitting, errors can arise from the neglected cross terms. In this paper, a higher-order split-step Fourier algorithm is proposed to reduce such errors, and their performance is demonstrated by solving two idealized ocean waveguide problems.

The one-way parabolic wave equation can be written as the following in terms of demodulated sound pressure $u(x, y, z)$ by removing the baseline phase according to the reference wavenumber k_0, i.e., $u(x, y, z) = p(x, y, z)\exp(-ik_0x)$, where p is sound pressure:

$$\frac{\partial}{\partial x}u(x,y,z) = ik_0\left\{-1+\sqrt{n^2(x,y,z)+k_0^{-2}\nabla_\perp^2}\right\}u(x,y,z), \tag{1}$$

where the Cartesian coordinate system is chosen to obtain a uniform resolution throughout the domain. In Eq. (1), n is the index of refraction with respect to k_0, and $\nabla_\perp^2 = (\partial^2/\partial y^2 + \partial^2/\partial z^2)$ is the two-dimensional (2D) Laplacian. To solve Eq. (1), the square-root Helmholtz operator $\sqrt{n^2+k_0^{-2}\nabla_\perp^2}$ will be approximated, and the approximation error will vary with azimuth angles. Our goal is to develop a higher-order

[a]Author to whom correspondence should be addressed.

approximation with a large valid angle so that the solution is accurate over a large domain. The Cartesian PE solution marches forward along a single direction, and the x axis of the coordinate system is aligned with that.

A brief review of the split-step Fourier PE theory is provided in the following. Tappert (1974b) applied the following linear approximation to the square-root Helmholtz operator for the split- step Fourier method to work:

$$\sqrt{1+\varepsilon+\mu} \cong 1+\frac{1}{2}\varepsilon+\frac{1}{2}\mu = Q_1, \tag{2}$$

where $\varepsilon = n^2 - 1$ and $\mu = k_0^{-2}\nabla_\perp^2$. It is shown that Tappert's approximation, denoted by Q_1, is valid within $\pm 10^\circ$ around the PE marching direction (Jensen *et al.*, 1994). A 3D implementation of Q_1 was performed by Martin and Flatté (1988) for optical waves propagating through random media. Another approximation with a valid angle range significantly greater than Tappert's was proposed by Feit and Fleck (1978), i.e.,

$$\sqrt{1+\varepsilon+\mu} \cong -1+\sqrt{1+\varepsilon}+\sqrt{1+\mu} = Q_2. \tag{3}$$

This approximation, denoted by Q_2, can also work with the split-step Fourier method, and it was first used by Thomson and Chapman (1983) for a wide angle 2D PE model in underwater acoustics. 3D implementations with Cartesian coordinates were made by Feit and Fleck (1978) in optics and by Duda (2006) in underwater acoustics. An approach employing a pressure variable $p/\sqrt{\rho}$ with interface smoothing was proposed by Tappert (1977) to handle density (ρ) discontinuity in split-step Fourier PE models. The effective index of refraction for the density-reduced pressure is shown as follows (Bergman, 1946):

$$\tilde{n}^2 = n^2 + \frac{1}{2k_0^2}\left[\frac{1}{\rho}\nabla^2\rho - \frac{3}{2\rho^2}(\nabla\rho)^2\right], \tag{4}$$

from which one can see that the anomaly of $\tilde{n}$ depends strongly on the sharpness of the interface smoothing and the sound frequency. Note that $k_0 = 2\pi f/c_0$, where f is the frequency and c_0 is the reference sound speed. In many shallow water problems of low frequency sound propagation, the anomaly of $\tilde{n}$ can be large when a sharp interface is needed. This causes the use of Q_1 or Q_2 to produce significant errors. An improved approximation to the square-root Helmholtz operator is proposed in Sec. 2 to handle greater refractive index anomalies.

2. Higher-order split-step Fourier algorithm

The operator $\sqrt{1+\varepsilon+\mu}$ can in fact be approximated into the following second-order Taylor series around $\sqrt{1+\varepsilon} = 1$ and $\sqrt{1+\mu} = 1$ to include two cross terms with ε and μ,

$$\begin{aligned}\sqrt{1+\varepsilon+\mu} \cong \sqrt{1+\varepsilon} + \left(-1+\sqrt{1+\mu}\right) - \frac{1}{2}\left(-1+\sqrt{1+\varepsilon}\right)\left(-1+\sqrt{1+\mu}\right) \\ -\frac{1}{2}\left(-1+\sqrt{1+\mu}\right)\left(-1+\sqrt{1+\varepsilon}\right) = Q_3,\end{aligned} \tag{5}$$

which is the new approximation used in this paper, denoted by Q_3. This approximation will reduce to Q_2 if the cross terms with ε and μ are neglected, and it will reduce to the higher-order approximation used by Yevick and Thomson (1994) when the operators $\sqrt{1+\varepsilon}$ and $\sqrt{1+\mu}$ in the cross terms are approximated to $1+\varepsilon/2$ and $1+\mu/2$, respectively. Here we follow Feit and Fleck (1978) to examine the approximation error defined as $\boldsymbol{E}_3 = (Q_3)^2 - (k_0^{-2}\nabla_\perp^2 + n^2)$. For 3D sound waves with a single wavenumber component, $p = \exp(i\vec{k}\cdot\vec{x})$, the error bound of $\boldsymbol{E}_3$ is found to be

$$|\boldsymbol{E}_3(\delta n, \gamma)| \le 2|\Delta n||\cos\gamma - 1|\,(|\Delta n| + |\cos\gamma - 1|), \tag{6}$$

where Δn is the refractive index anomaly from unity, and γ is the angle between the wavenumber vector $\vec{k}$ and the PE marching direction. Figure 1 shows a comparison to the error bounds of the other two approximations Q_1 and Q_2 found by Thomson and Chapman (1983), and it is clear that Q_3 can handle larger propagation angles and greater anomalies.

The finite-difference solution of the parabolic wave equation (1) using the approximation Q_3 is $u(x+\Delta x) = e^{\delta[\mathcal{L}+\mathcal{N}-(\mathcal{N}\mathcal{L}+\mathcal{L}\mathcal{N})/2]}u(x) + \tilde{E}$, where $\delta = ik_0\Delta x$, and two new notations are defined for operators $\mathcal{N} = -1 + \sqrt{1+\varepsilon} = n - 1$ and $\mathcal{L} = -1 + \sqrt{1+\mu} = -1 + \sqrt{1+k_0^{-2}\nabla_\perp^2}$. In the PE solution, the error $\tilde{E}$ is due to an assumption that the environment does not vary in each marching step from x to $x + \Delta x$. Using a Taylor series expansion, we can find $\tilde{E} = 0.5(\Delta x)^2 ik_0[\mathcal{N}_x - (\mathcal{N}_x\mathcal{L} + \mathcal{L}\mathcal{N}_x)/2]u(x) + O\left((\Delta x)^3\right)$, where $\mathcal{N}_x$ is the derivative of $\mathcal{N}$ with respect to x, and this error $\tilde{E}$ will entirely vanish when $\mathcal{N}_x = 0$, leaving only approximation errors from Q_3. To implement the PE solution, we actually use the following exponential operator splitting:

$$e^{\delta[\mathcal{L}+\mathcal{N}-(1/2)(\mathcal{N}\mathcal{L}+\mathcal{L}\mathcal{N})]} = e^{\delta(\mathcal{L}/2)}e^{\delta\mathcal{N}}e^{-(\delta/2)(\mathcal{N}\mathcal{L}+\mathcal{L}\mathcal{N})}e^{\delta(\mathcal{L}/2)} + \frac{\delta^2}{4}[\![\mathcal{N}, (\mathcal{N}\mathcal{L}+\mathcal{L}\mathcal{N})]\!] + O(\delta^3), \tag{7}$$

where the square brackets denote $[\![\mathcal{A}, \mathcal{B}]\!] = \mathcal{A}\mathcal{B} - \mathcal{B}\mathcal{A}$, which is a measure of non-commutativity between $\mathcal{A}$ and $\mathcal{B}$. Although this operator splitting is second order in δ, its error term has only the derivative operator $\mathcal{L}$ to its first power, which makes this method robust. Note that the non-commutative error is proportional to the gradient of the refractive index, so it requires interface smoothing and small marching steps to reduce the error.

To solve the cross operator with $\mathcal{N}$ and $\mathcal{L}$ in Eq. (7), we expand it into a Taylor series with a small δ,

$$e^{-(\delta/2)(\mathcal{N}\mathcal{L}+\mathcal{L}\mathcal{N})} = 1 + \sum_{m=1}^{\infty}\frac{1}{m!}\left[-\frac{\delta}{2}(\mathcal{N}\mathcal{L}+\mathcal{L}\mathcal{N})\right]^m, \tag{8}$$

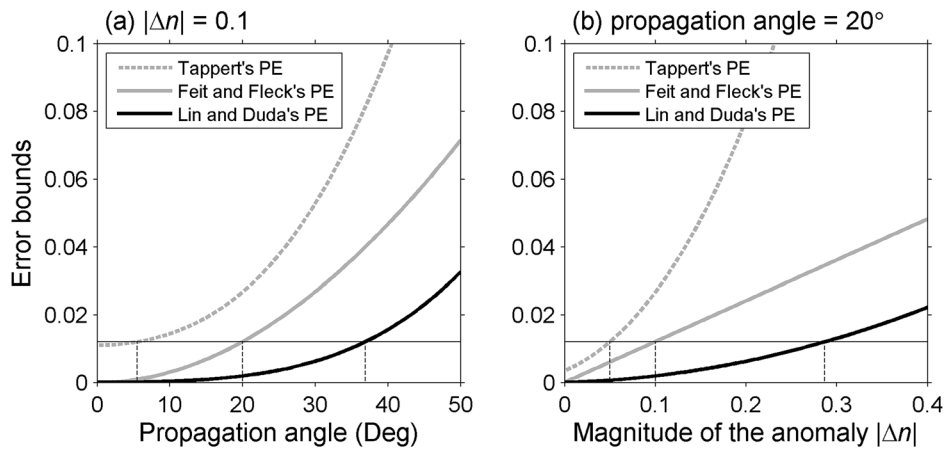

Fig. 1. Comparisons of the PE approximation errors. Thomson and Chapman (1983) showed that Tappert's and Feit and Fleck's approximations, Q_1 and Q_2, have the following error bounds, $|\boldsymbol{E}_1(\Delta n, \gamma)| \le [|\Delta n|(2 + |\delta n|) + \sin^2\gamma]^2/4$, and $|\boldsymbol{E}_2(\Delta n, \gamma)| \le 2|\Delta n||\cos\gamma - 1|$, respectively.

which may be calculated to a limited order M depending on the level of precision required. Then, the PE solution can be determined in the following steps:

$$\Delta u_1 = -\frac{\delta}{2}(\mathcal{N}\mathcal{L} + \mathcal{L}\mathcal{N})e^{\delta(\mathcal{L}/2)}u(x), \tag{9a}$$

$$\Delta u_m = -\frac{\delta}{2m}(\mathcal{N}\mathcal{L} + \mathcal{L}\mathcal{N})\ \Delta u_{m-1} \quad \text{for } m > 1, \tag{9b}$$

$$u(x + \Delta x) = e^{\delta(\mathcal{L}/2)}e^{\delta\mathcal{N}}\left[\sum_{m=1}^{M}\Delta u_m + e^{\delta(\mathcal{L}/2)}u(x)\right], \tag{9c}$$

where the cross-term corrections to $u(x)$ are first calculated with Eqs. (9a) and (9b), and they are used in Eq. (9c) to determine $u(x + \Delta x)$. The number of the iterations in Eq. (9c) depends on the required precision. In the numerical examples shown in the following, $|\Delta u_m|/|u|$ always converges to 1×10^{-6} within five iterations or less. Finally, since both the differential operators $\mathcal{L}$ and $e^{\delta\mathcal{L}}$ can be implemented with Fourier transforms, this higher-order PE method shares the same advantage as the original split-step Fourier PE method in fast computation of the 2D second-order derivatives. Implementation of $\mathcal{L}$ and $e^{\delta\mathcal{L}}$ with Fourier transforms are shown in the following:

$$\mathcal{L}u(x) = \left(-1 + \sqrt{1 + k_0^{-2}\nabla_\perp^2}\right)u(x) = \mathcal{F}^{-1}\left\{-1 + \sqrt{1 - (|\vec{k}_\perp|/k_0)^2}\mathcal{F}\{u(x)\}\right\}, \tag{10a}$$

$$e^{\delta\mathcal{L}}u(x) = e^{i\Delta x(-k_0 + \sqrt{k_0^2 + \nabla_\perp^2})}u(x) = \mathcal{F}^{-1}\left\{e^{i\Delta x(-k_0 + \sqrt{k_0^2 - |\vec{k}_\perp|^2})}\mathcal{F}\{u(x)\}\right\}, \tag{10b}$$

where $|\vec{k}_\perp| = \sqrt{k_y^2 + k_z^2}$ is the magnitude of the transverse wavenumber vector.

When implementing the higher-order split-step Fourier PE model, an approach using artificial absorption layers (Jensen *et al.*, 1994) can be employed to imitate the radiation boundary condition, and the PE solution within the artificial layers should be discarded. Note that the absorption coefficients of the artificial layers should only be added to the operator $e^{\delta\mathcal{N}}$ in Eq. (9c). Also, interface smoothing is needed to reduce the anomaly of $\tilde{n}$ in Eq. (4) as well as the operator splitting error in Eq. (7). A hyperbolic tangent smoothing procedure (Tappert, 1977) is suggested here, and the formula for smoothing the discontinuity of density is

$$\rho(z) = \rho_W + 0.5(\rho_B - \rho_W)\left[1 + \tanh\left(\frac{z - D}{2d}\right)\right], \tag{11}$$

where ρ_W and ρ_B are the water and bottom densities, respectively, D is water depth, and d is the one-side halfway width for the smoothing. It may require a convergence test to determine the smoothing width d. We can use Eq. (4) to check the anomaly of $\tilde{n}$ for a given smoothing width and examine the accuracy of the approximation Q_3. We then determine Δx to reduce the non-commutative error in Eq. (7) and ensure the convergence of Eq. (8). It will be shown that Q_3 can in fact handle a smoothed density interface with the width d down to the order of 1/15th of the acoustic wavelength, and so the model error associated with the interface smoothing becomes insignificant.

3. Numerical examples

The first example is the 2D Pekeris waveguide problem with a constant water depth 200 m and a 75 Hz point source located at depth 100 m. The water column is homogeneous with sound speed 1500 m/s, density 1 g/cm^3, and no medium absorption. The

bottom is also homogeneous with sound speed 1700 m/s, density 1.5 g/cm^3, and medium absorption 0.5 dB/wavelength. In the PE calculation, a wide angle starter (Thomson and Bohun, 1988) is used to simulate the point source. It is also found that the PE solution with the new approximation Q_3 is not so sensitive to the reference sound speed c_0, and the example shown here uses $c_0 = 1450$ m/s.

This 2D Pekeris waveguide example is to demonstrate that the higher-order split-step Fourier PE can handle a sharp interface, and it is found that the density smoothing width d can go down to 1.25 m, which is 1/15th of the acoustic wavelength in the water, without suffering from large approximation errors. There is no need for sound speed smoothing at this frequency. The PE solution converges when the depth grid size Δz is 1 m and the marching step Δx is 1.25 m. The transmission loss (TL) solution from the higher-order PE model is compared to the reference normal mode solution, and the agreement is very good as shown in Fig. 2. On the other hand, the regular split-step PE model employing Q_2 without considering the cross terms with ε and μ is less accurate because it cannot handle the sharp interface given by the density smoothing procedure in the current case.

The second example tests how the new PE model handles the horizontal refraction. An idealized wedge problem is considered, and its geometry is shown in Fig. 3(a). The slope angle is 5°, and the medium properties follow the Pekeris waveguide example. A 75 Hz point source is located 2 km away from the wedge apex at 100 m depth. In the PE calculation, a 3D wide angle starter generalized from a 2D starter by Thomson and Bohun (1988) is used. The cross-range grid size Δy is 1.5 m, and the depth grid size Δz is 1 m. It is found that the PE model can handle density interface smoothing with the width $d = 1.25$ m, as in the Pekeris waveguide example, and its solution converges when the marching step Δx is 1.25 m.

The higher-order PE TL solution on the horizontal x–y plane at $z = 30$ m is shown in Fig. 3(b), and the interference structure caused by the horizontal refraction of normal modes is observable. The caustics of the first five vertical modes are calculated using a normal mode approach (Buckingham, 1987) and superimposed on the TL contours in Fig. 3(b). It is shown that the outermost border of the PE TL solution follows the first modal caustic predicted by the modal approach. Also, the vertical interference structure shown in Fig. 3(c) confirms that the cutoff ranges of modes 2–5 at $y = 0$ seen in the PE solution agree with the theoretical locations of the modal caustics. A method of images by Deane and Buckingham (1993) is used here to produce a reference solution, and it verifies the accuracy of the higher-order PE solution, see Fig. 3(d). The regular split-step Fourier (SSF) PE solution obtained from Q_2, which neglects the cross terms, is also shown in Fig. 3(d) for a comparison. Because the regular SSF method cannot handle the sharp interface smoothing ($d = 1.25$ m) applied here,

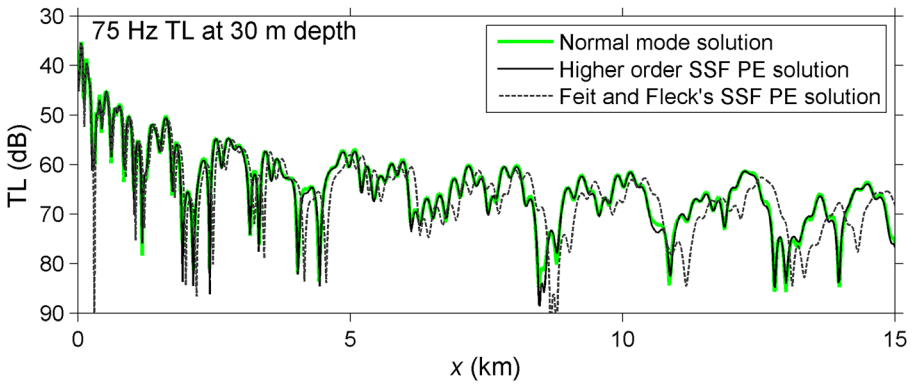

Fig. 2. (Color online) A model comparison for the Pekeris waveguide example. The higher-order SSF PE solution agrees with the reference normal modal solution very well, but not the regular SSF PE solution.

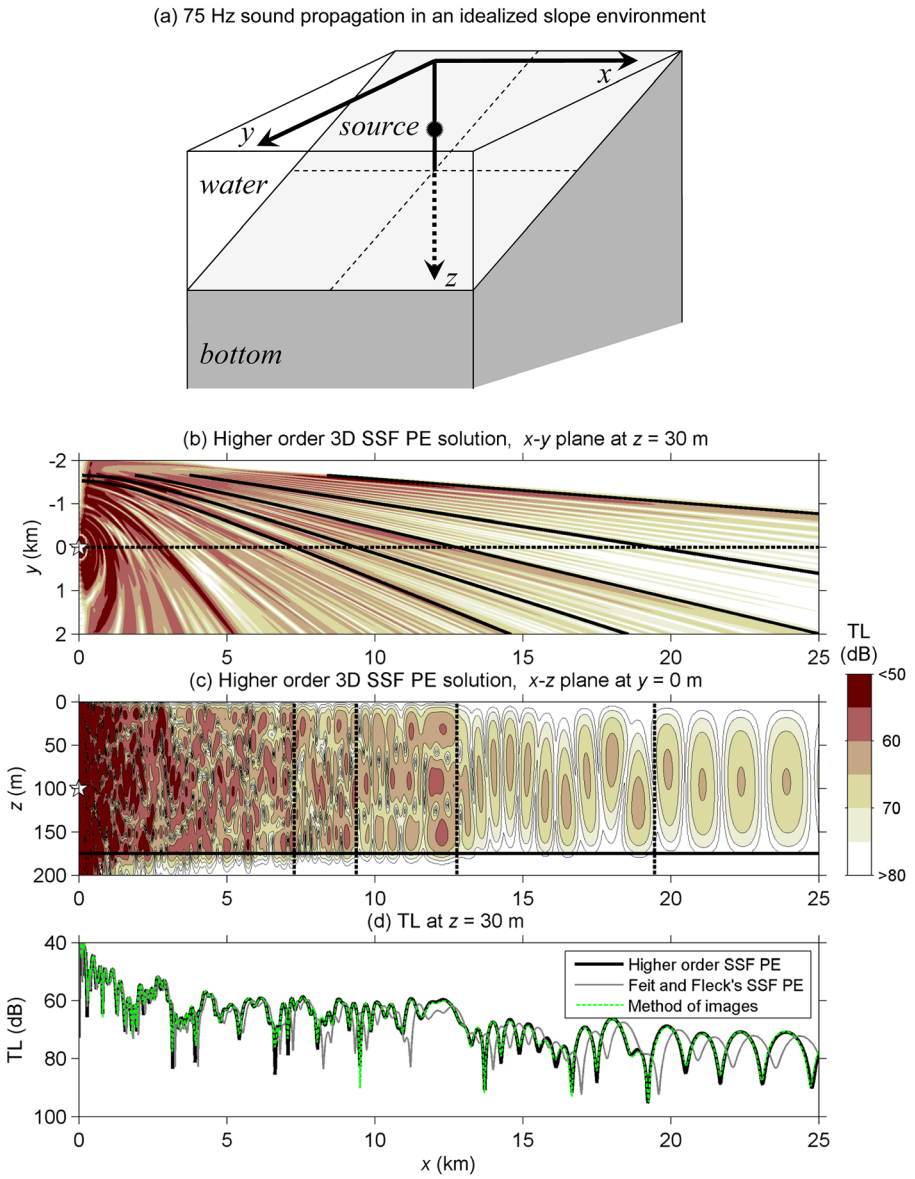

Fig. 3. (Color online) (a) Geometry of the idealized wedge example. (b) TL contours on the horizontal x–y plane at depth 30 m. (c) TL contours on the vertical x–z plane along $y = 0$. The solid lines in (b) are the hyperbolic loci of the first five modal caustics predicted by a modal theory (Buckingham, 1987), and the dashed lines in (c) denote the theoretical cutoff locations of modes 2–5. (d) Excellent agreement between the higher-order PE and a method of images.

its solution contains significant phase errors and starts deviating from the reference solution at about $x = 5$ km. On the other hand, the higher-order SSF method produces a solution matching with the image solution very well.

4. Summary

An improved SSF PE model with Cartesian coordinates is presented in this paper, and it employs a higher-order approximation to the square-root Helmholtz operator

$\sqrt{n^2 + k_0^{-2}\nabla_\perp^2}$. Since two cross terms with n and $\nabla_\perp^2$ are included, this PE model can handle larger propagation angles and greater refractive index anomalies comparing to the regular SSF PE.

The advantage of the presented higher-order SSF PE is appreciable when applying to 3D problems, because it utilizes the efficient fast Fourier transform to implement the Laplacian, 2D second-order spatial derivatives. Also, because the Laplacian is not split, the horizontal refraction is handled in the same order as the vertical refraction. The small marching steps might prevent the current theory from routine usage, but this higher-order SSF PE does provide a means to quantify the errors that the regular SSF PE will produce. Solving the PE solution with the cross terms in larger marching steps is proposed for future research.

Acknowledgments

This work was sponsored by the Office of Naval Research under Grants No. N00014-10-1-0040 and No. N00014-11-1-0701.

References and links

Bergman, P. G. (**1946**). "The wave equation in a medium with a variable index of refraction," J. Acoust. Soc. Am. **17**, 329–333.

Buckingham, M. J. (**1987**). "Theory of three dimensional acoustic propagation in a wedgelike ocean with a penetrable bottom," J. Acoust. Soc. Am. **82**, 198–210.

Deane, G. B., and Buckingham, M. J. (**1993**). "An analysis of the three-dimensional sound field in a penetrable wedge with a stratified fluid or elastic basement," J. Acoust. Soc. Am. **93**, 1319–1328.

Duda, T. F. (**2006**). "Initial results from a Cartesian three-dimensional parabolic equation acoustical propagation code," Woods Hole Oceanographic Institution Technical Report No. WHOI-2006-041, available at http://hdl.handle.net/1912/1428 (Last viewed 6/19/2012).

Feit, M. D., and Fleck, J. A., Jr. (**1978**). "Light propagation in graded-index fibers," Appl. Opt. **17**, 3990–3998.

Jensen, F. B., Kuperman, W. A., Porter, M. B., and Schmidt, H. (**1994**). *Computational Ocean Acoustics* (AIP, New York), Chap. 6.

Martin, J. M., and Flatté, S. M. (**1988**). "Intensity images and statistics from numerical simulation of wave propagation in 3-D random media," Appl. Opt. **27**, 2111–2126.

Tappert, F. D. (**1974a**). "Numerical solutions of the Korteweg-de Vries equation and its generalizations by the split-step Fourier method," in *Nonlinear Wave Motion*, edited by A. C. Newell, Lectures in Applied Mathematics Vol. 15 (American Mathematical Society, New York), pp. 215–216.

Tappert, F. D. (**1974b**). "Parabolic equation method in underwater acoustics," J. Acoust. Soc. Am. **55**, S34.

Tappert, F. D. (**1977**). "The parabolic equation method," in *Wave Propagation and Underwater Acoustics*, edited by J. B. Keller and J. Papadakis, Lecture Notes in Physics Vol. 70 (Springer, New York), pp. 224–286.

Thomson, D. J., and Bohun, C. S. (**1988**). "A wide-angle initial field for parabolic codes (A)," J. Acoust. Soc. Am. **83**, S118.

Thomson, D. J., and Chapman, N. R. (**1983**). "A wide-angle split-step algorithm for the parabolic equation," J. Acoust. Soc. Am. **74**, 1848–1854.

Yevick, D., and Thomson, D. J. (**1994**). "Split-step/finite-difference and split-step/Lanczos algorithms for solving alternative higher-order parabolic equations," J. Acoust. Soc. Am. **96**, 396–405.